species are produced by a reaction similar to (1), namely,

$$Xe+h\nu \rightarrow Xe^*$$

followed by (2)

$$Xe^*+Xe \rightarrow Xe_2^* \rightarrow Xe_2^+ + e + KE.$$

Reaction (2) has been verified in the case of the alkali metals.[7–11]

The many-lined spectrum of molecular hydrogen was used as a photon source, while dispersion of the radiation was achieved by a ½-m Seya monochromator with a wavelength resolution of 0.7 Å. A windowless ion chamber with a pathlength of 28 cm was employed to investigate the ionization resulting from resonance-line absorption by both xenon and krypton, although a lithium fluoride window was used at higher xenon pressures to study the direct excitation and ionization of Xe_2. Research-grade gas was used at pressures ranging from 1 to 300 torr. Ion currents of the order of 10^{-12} A were obtained at wavelengths corresponding to the following resonance-line absorptions with $\Delta J=1: mp^6\,{}^1S \rightarrow nd'[3/2]°$, $(n+1)d[3/2]°$, $(n+2)s'[1/2]°$, and $(n+3)s[3/2]°$, where for Xe, $n=5, 6, \cdots$ etc. and $m=5$; for Kr, $n=4, 5, \cdots$ etc. and $m=4$. At higher pressures, ionization was observed to occur at wavelengths lying between resonance lines and is attributed to either direct ionization of the rare gas molecule or excitation of the molecule followed by an autoionizing transition into the continuum state of the molecular ion.

Ions first appeared at 963.37 Å in krypton corresponding to the $4p$–$5d$ resonance transition. Thus, assuming reaction (2) is applicable, the ionization potential of Kr_2 would be ≤ 12.87 eV (963.37 Å). Melton and Hamill[5] obtained an appearance potential of 13.2±0.02 eV while Hornbeck and Molnar[3] quote a value of $13.23_{-0.7}^{+0.3}$ eV.

In the case of xenon, the first resonance transition which produced ionization was the $5p-6d$ transition at 1110.71 Å. However, the appearance potential of ions at high pressure (10 to 100 torr) was at 1112.7±2 Å. Thus, it is concluded that the ionization potential of Xe_2 is 11.14±0.02 eV (1112.7±2 Å).

The dissociation energy of the ground state of Xe_2^+ is, therefore, 0.99±0.02 eV; for Kr_2^+, the dissociation energy is ≥ 1.13 eV.

[1] O. Tuxen, Z. Physik 103, 463 (1963).
[2] F. L. Arnot and M. B. McEwen, Proc. Roy. Soc. (London) A-166, 543 (1938).
[3] J. A. Hornbeck and J. P. Molnar, Phys. Rev. 84, 621 (1951).
[4] F. H. Field, Harlan N. Head, and J. L. Franklin, J. Am. Chem. Soc. 84, 1118 (1962).
[5] C. E. Melton and W. H. Hamill, J. Chem. Phys. 41, 1469 (1964).
[6] R. K. Curran, J. Chem. Phys. 38, 2974 (1963).
[7] F. Mohler, P. Foote, and R. Chenault, Phys. Rev. 27, 37 (1926).
[8] E. O. Lawrence and N. Edlefsen, Phys. Rev. 34, 233 (1929).
[9] F. Mohler and C. Boeckner, J. Res. Natl. Bur. Std. 5, 51 (1930).
[10] K. Freudenberg, Z. Physik 67, 417 (1931).
[11] Y. Lee and B. H. Mahan, J. Chem. Phys. 42, 2893 (1965).

Spatial and Temporal Contrast-Sensitivity Functions of the Visual System

J. G. Robson
Physiological Laboratory, Cambridge, England

(Received 3 March 1966)

Index Heading: Vision.

The dependence of the form of the spatial contrast-sensitivity function for a square-wave test grating upon the duration of exposure of the target has been investigated by Schober and Hilz.[1] Kelly[2] has pointed out an analogous dependence of the form of the temporal contrast (modulation) sensitivity function upon the angular extent of the test target. The reciprocal nature of these spatio-temporal interactions can be particularly clearly appreciated if the threshold contrast is determined for a grating target whose luminance perpendicular to the bars is given by

where m is the contrast, ν the spatial frequency, and f the temporal frequency of the target.

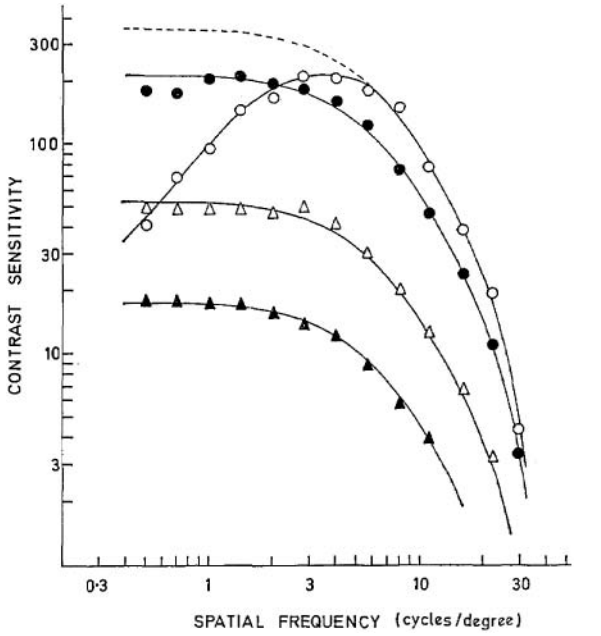

Fig. 1. Spatial contrast-sensitivity (reciprocal of threshold contrast) functions for different temporal frequencies. The points are the means of four measurements and the curves (one with a dashed low-frequency section) differ only in their positions along the contrast-sensitivity scale ○ 1 cycle per second, ● 6, △ 16, ▲ 22 cycles per second.

Such a pattern was set up as a display on a cathode-ray oscilloscope and Figs. 1 and 2 show the results of threshold-contrast measurements made by the author (a well-corrected myope). Viewing was binocular at a distance of 2 m. The grating pattern subtended 2.5°×2.5° in the center of a 10°×10° screen illuminated to the same mean luminance of 20 cd/m².

The general similarity of the two sets of contrast-sensitivity functions is immediately evident but two features are particularly remarkable. First, the form of the fall-off in sensitivity at high

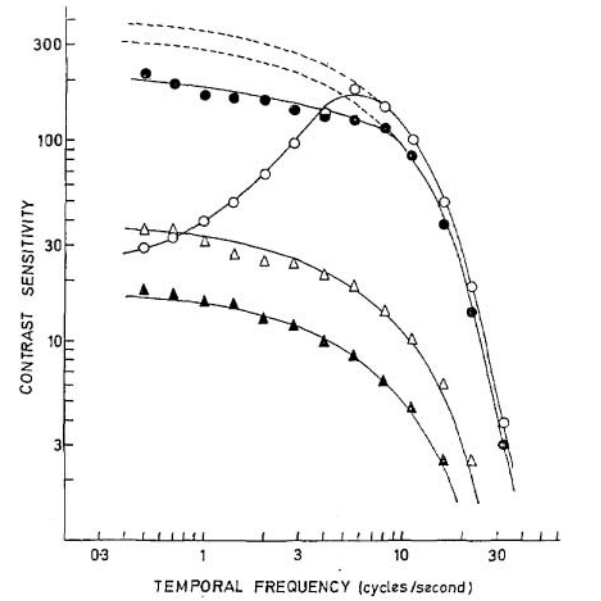

Fig. 2. Temporal contrast-sensitivity (reciprocal of threshold contrast) functions for different spatial frequencies. The points are the means of four measurements and the curves (two with dashed low-frequency sections) differ only in their positions along the contrast-sensitivity scale, ○ 0.5 cycle per degree, ● 4, △ 16, ▲ 22 cycles per degree.

spatial frequencies is independent of the temporal frequency and vice versa. Second, a fall-off in sensitivity at low spatial frequencies occurs only when the temporal frequency is also low and vice versa.

The first of these findings implies that the attenuation of high spatial frequencies is provided either entirely by an optical mechanism or partially by an optical mechanism and partially by a process of spatial integration in the nervous system that occurs effectively instantaneously.[1] The second finding is consistent with the suggestion[2,3] that the fall-off in sensitivity at both low spatial and low temporal frequencies is the result of an antagonism between signals from the center and surround regions of receptive fields. Since the surround region of a receptive field has a greater diameter than the center region, signals from the surround are relatively more attenuated at high spatial frequencies than signals from the center. Thus at high spatial frequencies the effect of the surround becomes negligible and the contrast-sensitivity is determined by the temporal characteristics of the center alone. But at high temporal frequencies also the effect of the surround appears to be negligible. Thus it must be assumed that some mechanism causes signals from the surround to be relatively more attenuated at high temporal frequencies than signals from the center.

[1] H. A. W. Schober and R. Hilz, J. Opt. Soc. Am. 55, 1086 (1955).
[2] D. H. Kelly, Doc. Ophthalmol. 18, 16 (1964).
[3] J. Levinson, Doc. Ophthalmol. 18, 36 (1964).

Underwater Holography

R. M. Grant, R. L. Lillie, and N. E. Barnett
The University of Michigan, Cooley Electronics Laboratory, Department of Electrical Engineering, Ann Arbor, Michigan 48104
(Received 8 April 1966)

Index Headings: Holography.

THIS letter reports the observation of holograms of objects immersed in water, using the well-known wavefront-reconstruction imaging technique.[1-4] Motivated by our objectives to study underwater acoustic vibrations, both for the purpose of pursuing new underwater acoustic detection techniques and analyzing acoustic vibrations of underwater objects by hologram reconstruction interferograms,[5] we set up the following experiment to determine, first of all if holograms could be made from objects immersed in water.

An object was placed in a water-filled glass tank and illuminated with coherent light from a Spectra Physics Model 115 He–Ne gas laser as shown in Fig. 1. An 8-mm microscope objective was used with a 25-μ diam pinhole, to provide a diverging beam. A portion

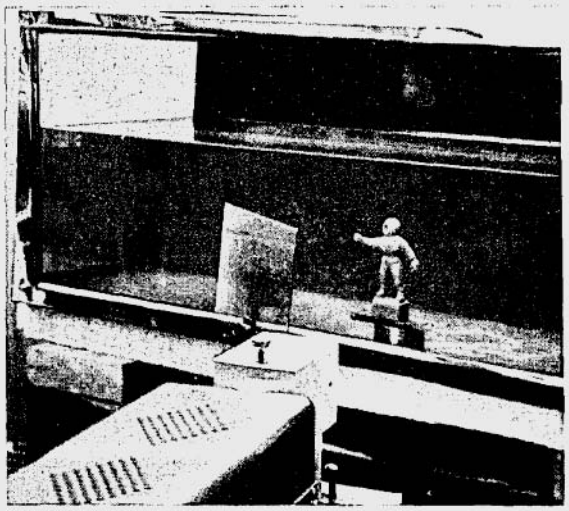

Fig. 1. Ordinary photograph of experimental setup.

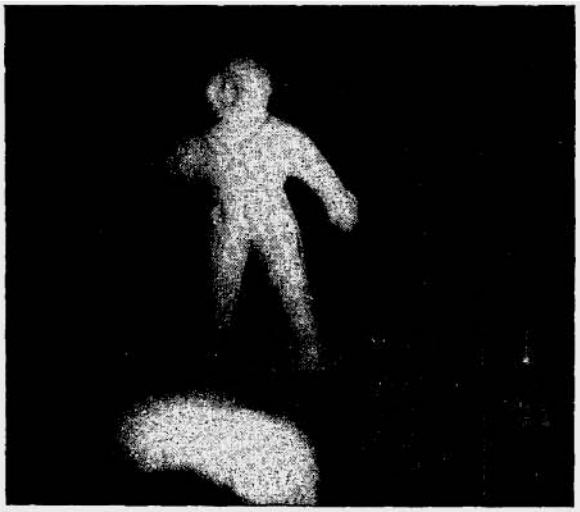

Fig. 2. Experimental results. Photograph of hologram-reconstructed image of diver under water (Laser beam directed through the hologram).

of the coherent light is diffusely reflected from the object in the water tank, retraverses the front face of the tank and falls upon an Eastman Kodak (type 649-F) photographic plate. This plate is also simultaneously illuminated by reflection from the front surface of the glass tank, which acts as a beam splitter. The result is a recording in the photographic emulsion of the interference pattern between the reference light reflected from the front of the tank and the light diffusely reflected from the object in the water. An exposure time of about three minutes yielded a reasonably good recording of the interference pattern. Reilluminating the plate with the reference beam produced clearly recognizable reproductions of the object in the water. (see Fig. 2).

The quality of the reconstructed image did not appear to be recognizably different from a reconstructed image of an object in air obtained in a similar way. Some minor deficiencies in equipment and technique are suspected of slightly degrading the quality of our holograms.

The above demonstration with objects in water suggests that holograms can be made with additional portions of the optical paths underwater including the photographic plate. Indeed, the entire arrangement shown in Fig. 1 might be immersed in water.

The above research has been supported in part by the U. S. Department of the Navy, Office of Naval Research, Acoustics Programs.

[1] D. Gabor, Nature 161, 777 (1948); Proc. Roy. Soc. (London) A197, 454 (1949).
[2] G. W. Stroke, *An Introduction to Optics of Coherent and Non-Coherent Electromagnetic Radiations* (The University of Michigan, Ann Arbor, 1964), 1st Edition.
[3] E. N. Leith and J. Upatnieks, Sci. Am. 212, (6) 24 (1965).
[4] E. N. Leith and J. Upatnieks, J. Opt. Soc. Am. 54, 1295 (1964).
[5] K. A. Stetson and R. L. Powell, J. Opt. Soc. Am. 55, 1570A (1965).